THE GENERATION OF INSTATIONARY FLOW CONDITIONS IN THE HIGH SPEED CASCADE WIND TUNNEL

Paola Acton, Leonhard Fottner

Institut für Strahlantriebe
Universität der Bundeswehr München
D-85577 Neubiberg

THE GENERATION OF INSTATIONARY FLOW CONDITIONS IN THE HIGH SPEED CASCADE WIND TUNNEL

Paola Acton, Leonhard Fottner
Institut für Strahlantriebe
Universität der Bundeswehr München
D-85577 Neubiberg
Germany

ABSTRACT

The flow in turbomachines is characterised by high turbulence levels as well as by strong non uniformity and instationarity. Each blade row generates wakes with lowered velocities and higher turbulence levels. The relative motion between rotor and stator rows gives rise to a non-uniform and instationary flow impinging on the downstream blade rows. This phenomenon strongly influences the boundary layer behaviour on the blade surfaces and hence the losses and the loading of the profile. Measurements in cascade wind tunnels with homogeneous inlet conditions have often shown inferior aerodynamic performances of the profiles to those obtained in a real turbomachine. For this reason the design of test facilities which enable measurements on large scale blades under non-uniform and instationary flow conditions helps to improve the quality of the prediction of the turbomachine performances enormously. Some low speed wind tunnels have already been equipped with wake generating mechanisms, but up to now no high speed wind tunnel has been provided with a wake generator.

In the High-Speed Cascade Wind Tunnel of the Universität der Bundeswehr München compressor and turbine cascades can be tested under conditions similar to real turbomachines, because Mach number and Reynolds number can be varied independently in a typical range. This facility has been equipped with a wake generator that can simulate a moving blade row in front of the linear cascade mounted in the test section. The wakes are generated by cylinders fastened to two parallel timing belts moving with a velocity of up to 60 m/s in front of and behind the tested cascade. The timing belts are driven by a variable speed AC-motor via a mechanism of transmission belts and pulleys.

Measurement techniques characterised by high frequency responses have been used in order to analyse the different unsteady phenomena separately. Hot wires and hot films give information about the variation of the boundary layer conditions along the blades during the wake passing period. The analysis of the raw data, of the mean values, and of the ensemble averaged data enables a deep insight in the phenomenon of transition on the blades under distorted inlet conditions.

NOMENCLATURE

Symbols:

c	[m/s]	velocity
$c_{p,v/l}$	[-]	pressure distribution coefficient
d	[mm]	bar diameter
E	[V]	anemometer output signal
f	[Hz]	frequency
f_s	[kHz]	sampling rate
F	[N]	centrifugal force
l	[mm]	chord length
N	[-]	number of samples
p	[Pa]	pressure
q	[Pa]	dynamic pressure
t	[s]	time
t	[m]	pitch
T	[s]	bar passing period
Tu	[%]	turbulence level
u	[m/s]	bar velocity
U	[m/s]	flow velocity in x direction
x	[mm]	coordinate in streamwise direction
β	[°]	flow angle
β_s	[°]	stagger angle
μ_3	[-]	skewness
μ_4	[-]	flatness
τ_w	[N/m²]	shear stress
ω	[-]	pressure loss coefficient

Subscripts and superscripts:

0	free convection conditions
1	upstream conditions
2	downstream conditions
2th	downstream conditions for isentropic flow
ax	axial
b	referring to the bars
k	related to the pressure tank of the wind tunnel
ref	reference conditions

t total conditions
∞ free stream conditions
~ ensemble averaged
' turbulent fluctuation

Abbreviations:

Ma Mach number
Re Reynolds number
So Strouhal number
EIZ generator of instationary flow conditions (Erzeuger Instationärer Zuströmbedingungen)
HGK High Speed Cascade Wind Tunnel (Hochgeschwindigkeits-Gitterwindkanal)
RMS Root Mean Square

INTRODUCTION

The design philosophy for modern turbomachines leads towards components with a smaller number of stages, characterised by higher loaded blades. This is particularly important for aviation gas turbines in order to be able to enhance the thrust-to-weight ratio. The actual design methods can predict the performance of the blades under stationary inlet flow conditions. The flow in a turbomachine however is characterised by strong instationarities, due to the wakes originating from the preceding blade row. The blade performance in the turbomachine can differ significantly from the one obtained from steady state calculations or from measurements in traditional wind tunnels.

The interaction between the wakes and the boundary layer along the blade surface can cause both an increment or a reduction of the losses across the blade row. The impinging wakes are characterised by higher turbulence levels and total pressure losses and can change the behaviour of the boundary layer transition causing the natural transition to move periodically further upstream and therefore inducing increased profile losses. If however the transition on the suction side of the blade is designed to occur via a separation bubble, the impinging wakes may suppress the separation bubble and hence reduce the profile losses.

The interest of the research towards this item has grown during the last few years. As it is difficult to perform measurements in real turbomachines because of their small dimensions the boundary layer development along large scale models was analysed in wind tunnels. It began with basic research about the influence of wakes on the boundary layer behaviour along flat plates and cylinders (*Schröder* (1985), *Pfeil et al.* (1983)). The wakes were generated by cylindrical bars of different diameters fixed to a rotating squirrel cage mounted in front of the test object. The influence of pressure gradient and curvature on the boundary layer development were analysed by *John et al.* (1994) on a curved plate with a similar wake generating system.

In the early 90s the first experiments on linear cascades with instationary inlet flow conditions were performed in low speed wind tunnels (*Addison et al.* (1989); *Banieghbal et al.* (1995); *Schobeiri et al.* (1995)). The results have enabled a deeper insight of the transition under unsteady inlet flow conditions. The wake-induced unsteady flow generates zones of a becalmed boundary layer on the profiles, which alternate with turbulent zones. The wake-induced transition is characterised by an intermittent region between the laminar part and the fully turbulent part of the boundary layer. The wakes may induce an earlier beginning and contemporary a later end of the transition than in the stationary case.

To the knowledge of the authors no high speed test facility has yet been equipped with a wake generator capable of simulating the rotor-stator interaction characteristic for a turbomachine component. Furthermore the option of varying the Reynolds number, the Mach number, and the wake parameters independently from each other opens further possibilities in the research of the boundary layer development on turbine and compressor blades.

EXPERIMENTAL SET UP

The High Speed Cascade Wind Tunnel

The High Speed Cascade Wind Tunnel (HGK) of the University of the Federal Armed Forces in Munich is an open loop facility which can operate continuously and reach Mach numbers up to Ma = 1.05 in the test section (Fig.1). As the wind tunnel is build inside a large pressure tank it is possible to vary the Mach number and the Reynolds number in the test section independently (see *Sturm et al.* (1985)) in order to simulate the flow conditions inside real turbomachines correctly.

The air is supplied by a six-stage axial compressor, driven by a 1.3 MW a.c. electric motor which is situated outside the pressure tank. The air flows through a diffuser into a settling chamber, where it is cooled down to an adjustable constant temperature (30°C to 60°C), through a turbulence generator and finally is accelerated in the nozzle before reaching the 300 mm wide, variable height test section.

The Moving-Bar Facility for the Generation of Instationary Flow Conditions

The rotor-stator interaction is simulated in the HGK by cylindrical rods moving in front of the cascade. As was shown by *Pfeil et al.* (1976) the far wake of a cylinder is

similar to that of an airfoil given that both cause the same total pressure losses. Both the velocity and the pitch of the bars can influence the interaction between wakes and profile boundary layer. While the diameter of the cylinders and the distance between the bars and the inlet plane of the cascade affect the width and the strength of the wakes impinging on the blade cascade.

In order to simulate the wakes of turbomachine bladings with the help of cylindrical bars in a wind tunnel several similarity parameters have to be met correctly. The width, the total pressure loss (i.e. the velocity deficit) and the maximum turbulence level in the wake have to be matched. This can be done by changing the diameter of the bars and the distance between the bars and the inlet plane of the cascade. Only two independent variables can be varied while three dependent quantities have to be matched. Therefore it will not be possible to fit all characteristics of the blade wakes and the rod wakes. For the first tests steel bars with a diameter of 2 mm have been chosen. First results of the measurements behind the wake generator will be discussed.

Furthermore the Strouhal number similarity also has to be taken into account. The Strouhal number is defined as: $So = (f \cdot l)/c_{ax}$, where f is a frequency, l a typical length (here the chord length) and c_{ax} the axial velocity. It reaches values around $So = 0.8$ in modern turbines. With a typical turbine stage inlet flow velocity of $c_{ax} = 80$ m/s, a chord of $l = 100$ mm and a bar pitch which can be varied between $t_b = 10$ and $t_b = 80$ mm, a bar velocity of $c_b = 6$ m/s up to $c_b = 52$ m/s has to be achieved in order to verify the Strouhal similarity. Therefore the wake generating facility has been designed in order to stand velocities up to 60 m/s and to allow a continuous adjustment of the velocity.

The wake generator has been projected with a special stress on modularity in order to allow a change in the different wake parameters with reasonably low effort. The working principle of the wake generator is based on cylindrical bars fastened to two rubber timing belts moving in front and behind of the cascade. The timing belts, having a length of 4000 mm, span over two main pulleys of the diameter of 400 mm positioned above and beneath the cascade (Fig.2). The distance between the trailing edge of the cascade and the returning bars is big enough not to disturb the flow in the blade passages and to allow the traversing of any kind of probe usually employed during the tests. Pulleys of big dimensions have been chosen in order to reduce the high centrifugal forces due to the deviation of the bars. For the highest design velocity and steel bars of 2 mm diameter the centrifugal force on the bars amounts to $F = 136$ N, which may cause a plastic deformation of the bars. In order to reduce the loading on the bars they are guided by two additional flat belts and two pulleys as is shown in Fig.3. The toothed disks and the four pulleys for flat belts are fastened to two main axes, which are fixed to a rigid frame, ensuring the stability of the whole wake generator. The mounting supports of the gear boxes are designed in order to enable the control of the belt tension and the parallelism of the two axes. All the pulleys are crowned in order to centre the belts automatically. The toothed disks are equipped with a lateral guidance to fix the position of the belts.

One main problem in the design of the wake generator consists in the vibrations of the bars due to the centrifugal forces caused by the deviation around the pulleys and to the drag forces in the inlet and outlet plane of the cascade. Here the air velocities reach values between 100 m/s and 200 m/s and the von Karman vortices behind the bars may induce resonant vibrations in the bars and in the belts. Eight additional pulleys (d=100 mm) (Fig.4) support both the upstream and the downstream section with the aim of reducing the vibrations, which may cause structural problems and modify the shape of the generated wakes.

The driving pulley is positioned on the lower main shaft and is connected with a timing belt to the a.c. electric motor using a 1:1 transmission ratio. The motor has a nominal maximum power of 17 kW at 3000 rpm. It is necessary to cool the motor with water because the whole wind tunnel is installed inside a pressure tank, which can be evacuated down to a pressure of 50 hPa, and the free convection in the rarefied air wouldn't be sufficient to cool the engine. The motor can turn in both directions in order to simulate the rotor-stator interaction of compressor as well as of turbine stages. The velocity of the motor can be digitally regulated with an accuracy of 0.1 rpm from 100 rpm to 3000 rpm continuously.

The design of the whole wake generator is based on a rigid frame (2000 mm x800 mm) consisting of welded I-profiles of steel (Fig.5). All main and secondary shafts as well as the electric motor are fixed on this frame. This design concept permits a relatively easy installation in the wind tunnel as well as the possibility of changing the inlet flow angle of the cascade with reasonably small effort.

As one part of the toothed belts moves inside the wind tunnel nozzle upstream of the cascade it was necessary to reduce the width of the test section in order to avoid disturbances of the inlet flow to the cascade. Therefore two wooden side walls were designed (Fig.6) following the concepts of *Cohen et al.* (1962). Thus the width of the test section was reduced to 170 mm setting the aspect ratio for the usually employed cascades to 1.7.

In order to perform an ensemble averaged analysis of the high frequency signals it is necessary to know the exact position of the bars with respect to the blades at any time. Therefore a trigger module was fixed to the main frame in order to detect the wake passing.

The measurements are very time consuming because of the large amounts of data which have to be stored. Therefore one half of the timing belts was equipped with bars of a different pitch than the other half, allowing for the observation of two flow conditions in one measurement cycle.

MEASUREMENT TECHNIQUES

Pneumatic Measurements

In the first evolutionary step of the new test facility total pressure losses and surface pressure distribution are measured as mean values. For the loss evaluation the total pressure p_{t2} is measured by a wedge probe traversed at 40% of the chord length downstream of the trailing edge plane of the cascade over a whole pitch. The total pressure p_{t1} should be measured downstream of the moving bars and upstream of the cascade. This measuring position however leads to measurement errors due to the non linear averaging of the pitot probe in the instationary flow behind the bars (*Weyer* (1980)). Therefore the pressure p_{t1} is measured upstream of the bars and the total pressure loss across the moving bars is calculated theoretically following *Schulte* (1995).

For the calculation of the total pressure losses of a turbine cascade a 1-D-mixed-out calculation (*Amecke* (1967)) is performed, leading to the total pressure loss coefficient:

$$\omega = \frac{p_{t1} - p_{t2}}{q_{2th}} \qquad (1)$$

The surface pressure measurements are performed at several static pressure tappings on the suction and on the pressure side. For turbines these measurements are evaluated in form of a dimensionless pressure distribution coefficient:

$$C_{p,x/l} = \frac{p(x/l) - p_k}{p_{t1} - p_k} \qquad (2)$$

Glue-On Hot-Film Sensors (or Surface-Mounted Hot-Film Gauges)

Surface-mounted hot-film gauges were glued on the suction and on the pressure side of the blades in order to analyse the development of the shear stress and of the boundary layer conditions along the profile. The theoretical background for operating such probes was first explained by *Ludwieg* (1949), then further developed by *Bellhouse et al.* (1966) and is based on the correlation between the heat transfer in the boundary layer and the shear stress on the wall. Although it is theoretically possible to calibrate the sensors no calibration was performed as it is rather laborious and not necessary in order to get the desired information about transition and separation phenomena of the boundary layer, as was shown by *Schröder* (1991). The DC signal of the anemometer results from the free convection of the overheated sensor (E_0) and from the forced convection. As the free convection of the overheated sensor changes slightly for each sensor, the DC anemometer signals are normalised by E_0 as follows:

$$\tau(x/l) \propto \frac{E - E_0}{E_0}$$

The location and the form of the transition can be efficiently detected with the help of the normalised RMS value of the anemometer signal.

For the present measurements hot-film arrays by MTU Munich were glued on the whole suction and pressure side of two adjacent blades. Each sensor consists of a 3 mm long, ultra-thin nickel film (0.4 µ) deposited on a 0.1 mm polyimide substrate. One array consists of up to 80 sensors spaced in 3 mm distance.

The measurements were performed with the help of a constant temperature DANTEC bridge of the type 55M01. The sensors were successively connected to the bridge by a multiplexer, which could switch between 48 single mode channels. They were overheated to a temperature of 100° C corresponding to a overheat ratio of 0.25. A total of 28 sensors were used during the first test measurements on the suction side and 24 on the pressure side.

Hot-Wire Boundary Layer Measurements

Boundary layer traverses can be performed by a single wired DANTEC subminiature BL probe of the type 55P15 connected to a constant-temperature-bridge of the type 55M01. The probe can be traversed automatically in 0.1 mm steps by two computer driven step motors. The sensor calibration is performed in the open test section of the HGK and a polynomial of 4th degree is used for the approximation of the calibration curve. The polynomial calibration was chosen because it is better suitable for the high velocity conditions of the HGK than the application of King's law.

The same technique was applied for the measurements in the wakes of the bars and of the blades.

DATA ACQUISITION AND PROCESSING

The data acquisition, the processing and the control of the stepper motors are fully automated and basing on two

separated computer systems for the pneumatic measurements and the hot-sensor measurements.

The stationary pressure measurements are performed by means of a PC-driven software WINPANDA, which was developed by *Ganzert et al.* (1996). The software controls the Scanivalves, the pressure transducer, the movements of the step motors, the data acquisition and storage and performs an on-line data processing and graphical representation of the results.

The hot-sensor measurement techniques are controlled by a HP 3565 work station, which is able to acquire up to three channels simultaneously with a maximum sample frequency for each channel of 260 kHz. The analog data are first filtered by an anti-aliasing filter and then digitised by a 14-bit A/D-converter. The data are recorded on a fast hard disk and then stored on a Magneto Optical Disk.

The high frequency data from the thermal anemometry measurements are analysed in the time domain as raw data as well as in the frequency domain with the help of an FFT routine. Furthermore the well established ensemble averaging technique has been applied. The ensemble average of a time-dependent quantity b is given by:

$$\tilde{b}(t) = \frac{1}{N} \cdot \sum_{j=1}^{N} b_j(t) \tag{3}$$

where N is the number of ensembles and the ensemble averaged RMS is given by:

$$\sqrt{\tilde{b}'^2(t)} = \sqrt{\frac{1}{N-1} \cdot \sum_{j=1}^{N} \left(b_j(t) - \tilde{b}(t) \right)^2} \tag{4}$$

Also the skewness (third-order moment)

$$\mu_3 = \frac{1}{\left(\tilde{b}(t)\right)^3} \cdot \frac{1}{N-1} \cdot \sum_{j=1}^{N} \left(b_j(t) - \tilde{b}(t) \right)^3 \tag{5}$$

and the flatness factor (fourth-order moment)

$$\mu_4 = \frac{1}{3 \cdot \left(\tilde{b}'^2(t)\right)^2} \cdot \frac{1}{N-1} \cdot \sum_{j=1}^{N} \left(b_j(t) - \tilde{b}(t) \right)^4 \tag{6}$$

have been calculated in order to get a deeper insight into the boundary layer characteristics.

In the case of the hot-film data b can be substituted by the shear stress τ_w and for the hot-wire measurements with the velocity. In this case the ensemble averaged RMS intensity of the velocity

$$\tilde{T}u(t) = 100 \cdot \frac{\sqrt{\tilde{u}'^2(t)}}{\bar{u}} \tag{7}$$

is not the "turbulence intensity" because it contains not only the random fluctuations of the flow but also the periodic change of the boundary layer conditions from turbulent to laminar and the slow wake-passing frequency.

As the hardware didn't allow to trigger the acquisition-system with an external trigger it was necessary to acquire the signal continuously using one channel for the trigger signal and another for the data from the sensor. This technique leads to an enormous amount of data, which are only partially necessary for the successive analysis. Therefore a post-processing routine was programmed in order to eliminate the surplus data, storing only the data corresponding to up to 6 wake passages.

As the time intervall of the trigger signal from the optical sensor is 0.05 ms, a very high logging rate is necessary for its detection. Hence a sampling frequency of f_s=65.5 kHz was chosen even if the response time of the sensors is much higher. Therefore the analogue signal from the sensor is filtered by a low-pass analogue filter before being digitised by the A/D-converter. In order to apply the ensemble averaged technique 300 ensembles were taken, each consisting of 3146 samples corresponding to 6 wake passages.

FIRST EXPERIMENTAL RESULTS

The Wake Generation

Prior to the cascade tests single wire probe measurements were performed in the free stream behind the wake generator in order to analyse the shape and intensity of the generated wakes. The probe was positioned in the centre of the test section and the bars were moved with four different velocities in front of it. The ensemble averaged results are shown in Fig.7 and Fig.8 for the two bar-pitches: t_b=40 mm and t_b=80 mm respectively. The inlet flow conditions correspond to the theoretical outlet flow conditions Ma_{2th}=0.40 and Re_{2th}=2·10^5 for the turbine cascade T106. In each figure the wakes for the two different bar velocities u=10 m/s and u=20 m/s are represented in separate diagrams in form of ensemble averaged quantities. On the abscissa the time is normalised with the wake passing period. On the ordinate the ensemble averaged RMS value of the velocity fluctuation and the ensemble averaged velocity are normalised with the corresponding free stream values.

The wakes behind the bars are very similar for all analysed bar velocities. For the bigger bar pitch a distinct range of

non disturbed flow is visible between the wakes. For higher bar velocities a stronger velocity deficit concurring with increased turbulence levels can be noticed. The distribution of the turbulence level is non symmetric and displays a double peak due to the fact that the bars don't move perpendicular to the main flow.

The shape of the wakes generated by the smaller pitch is represented in Fig.8. Again the wake form is similar for both bar velocities while the intensity of the wake increases with increasing bar velocity. The undisturbed free stream flow has almost vanished because the wakes tend to join in the cascade inlet plane.

Hot-Film Measurements on the Suction Side of a Highly Loaded Turbine Profile - Exemplarly Results

The tests were performed on the highly loaded low pressure turbine profile T106. The design conditions and the geometry of the cascade are shown in Fig.9. Hot film measurements were performed at the design inlet flow angle β_1=127.7° for Ma_{2th}=0.40 and Re_{2th}=2·10^5. The velocity of the bars was set to u=40 m/s leading to a Strouhal number of So=0.67. The normalised ensemble averaged values of the anemometer signal and of its RMS value are plotted in form of a distance-time diagram in Fig.10 and Fig11 where the abscissa shows the normalised position along the blade surface and the ordinate the time divided by the wake passing period. Three wake passing periods are shown in the figures. The similarity of the results for the wakes of three different bars testifies the accuracy of the simulation of the rotor-stator interaction in the linear cascade. Near the leading edge of the blade a higher RMS value of the shear stress can be noticed corresponding to the impinging wakes. Along the suction side however these high fluctuations are damped because of the steady acceleration of the flow. Further downstream the root mean square value of the hot film sensor signals shows a maximum in correspondence to the transition point. The transition point moves between x/l = 0.73 and x/l = 0.80 depending on the relative position of the bars and the leading edge of the blade. This boundary layer behaviour is confirmed in Fig.11, where the normalised DC anemometer signal corresponds to the shear-stress along the blade surface. The position of the signal minimum is in good agreement with the location of the maximum gradient of the RMS values as was expected from previous measurements in stationary flow conditions.

SUMMARY

A new wake generator facility (EIZ) for the High-Speed Cascade Wind Tunnel has been developed, built and successfully tested. It is the first facility enabling measurements in a high speed wind tunnel under instationary conditions similar to those of real turbomachines. The Mach number, the Reynolds number and the velocity and intensity of the wakes can be varied independently. Velocity and turbulence measurements have been performed behind the bars to ascertain the wake shape. The boundary layer behaviour under periodically disturbed flow conditions was observed on a highly loaded low pressure turbine profile with the help of hot film sensors. The results show a good operativeness of the newly designed generator of instationary flow conditions and of the employed measurement techniques and data processing.

REFERENCES

Addison, J.S., Hodson, H.P. (1989), "Unsteady Transition in an Axial Flow Turbine. Part 2-Cascade Measurements and Modelling", ASME Paper 89-GT-290

Amecke, J. (1967), "Auswertung von Nachlaufmessungen an ebenen Schaufelgittern", Bericht 67A49, AVA Göttingen

Banieghbal, M.R., Curtis, E.M., Denton, J.D., Hodson, H.P., Hunstman, I., Schulte, V., Harvey, N.W., Steele, A.B. (1995), "Wake Passing in LP Turbine Blades", AGARD CP571

Bellhouse, B.J., Schultz, D.L. (1966), "Determination of Mean and Dynamic skin Friction, Separation and Transition in Low-Speed Flow with a Thin-film heated element", J. of Fluid Mech. Vol. 24, part 2, pp.:379-400

Cohen, M.J., Ritchie, N.J.B. (1962), "Low-Speed Three-Dimensional Contraction Design", J. of the Royal Aeronautical Society, Vol. 66, pp.:231-236

Ganzert, W., Fottner, L. (1996), "WINPANDA - an Enhanced PC-Based Data Acquisition System for Wake and Profile Distribution ", 13th Symp. on Meas. Tech. for Transonic and Supersonic Flows in Cascades and Turbo-machines, Zürich

John, J., Schobeiri, M.T. (1994), "Development of Two-Dimensional Turbulent Wakes in a Curved Channel at Positive Streamwise Pressure Gradients", ASME Paper 94-GT-384

Ludwieg, H. (1949), "Ein Gerät zur Messung der Wand-schubspannung turbulenter Reibungsschichten", Ingenieur Archiv, Band 17, pp.:207-218

Pfeil, H., Eifler, J. (1979), "Turbulenzverhältnisse hinter rotierenden Zylindergittern", Forschung im Ingenieur-wesen, Vol.42, pp.:27-32

Pfeil, H., Herbst, R, Schröder, Th. (1983), "Investigation of the Laminar-Turbulent Transition of Boundary Layers Disturbed by Wakes", J. of Engineering for Power, Vol. 105, pp.:130-137

Schobeiri, M.T., Pappu, K, Wright, L. (1995), "Experimental Study of the Unsteady Boundary Layer Behaviour on a Turbine Cascade", ASME Paper 95-GT-435

Schröder, Th., (1985), "Entwicklung des instationären Nachlaufs hinter quer zur Strömungsrichtung bewegten Zylindern und dessen Einfluß auf das Umschlagverhalten von ebenen Grenzschichten stromabwärts angeordneter Versuchskörper", Dissertation TH Darmstadt

Schröder, Th., (1991), "Investigation of the Blade Interaction and Boundary Layer Transition Phenomena in a Multistage Aero Engine Low-Pressure Turbine by Measurements with Hot-Film Probes and Surface-Mounted Hot-Film Gauges", Boundary Layers in Turbomachines, VKI Lecture Series 1991-6

Sturm, W., Fottner, L. (1985), "The High-Speed Cascade Wind Tunnel of the German Armed Forces University Munich", 8th Symp. on Meas. Tech. for Transonic and Supersonic Flows in Cascades and Turbomachines, Genoa

Schulte, V. (1995), "Unsteady Separated Boundary Layers in Axial-Flow Turbomachinery", A Dissertation submitted for the Degree of Doctor of Philosophy

Weyer, H.B. (1973), "Bestimmung der zeitlichen Druckmittelwerte in stark fluktuierender Strömung insbesondere in Turbomaschinen", Dissertation RWTH Aachen

test section data:

- Mach number : $0.2 \leq Ma \leq 1.05$
- Reynolds number : $10^6 \leq Re/l \leq 1.5 \cdot 10^7$
- degree of turbulence : $0.3\% \leq Tu_1 \leq 6\%$
- upstream flow angle : $25° \leq \beta_1 \leq 155°$
- blade height : 300 mm

wind-tunnel data:

- a.c. electric motor : P = 1300 kW
- axial compressor (six stages):
  - air flow rate : $V = 30\ m^3/s$ (max.)
  - total pressure ratio : $\Pi = 2.14$ (max.)
  - rotational speed : n = 6200 rpm (max.)
- tank pressure : $0.05\ bar \leq p_k \leq 1.2\ bar$

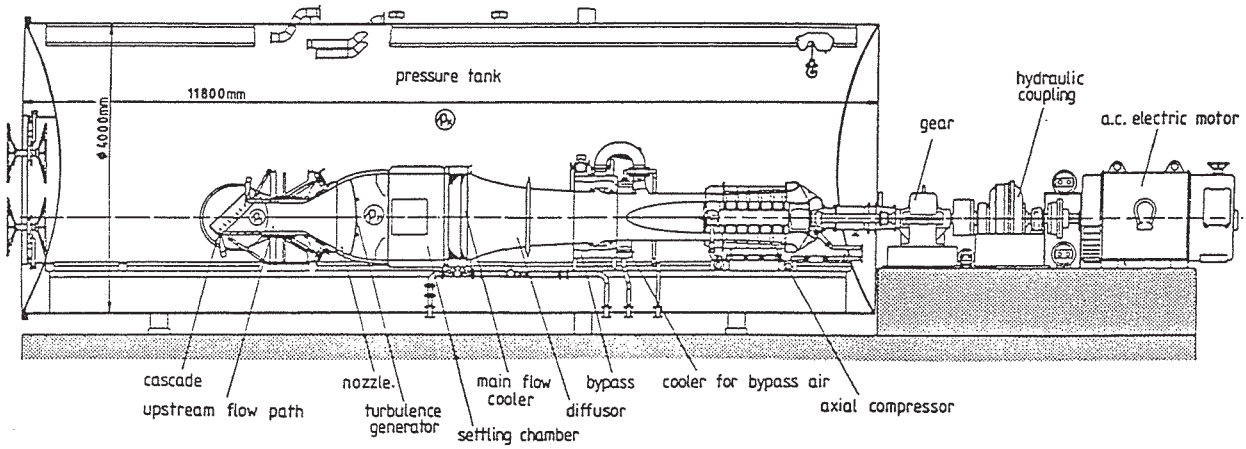

Fig.1 The High-Speed Cascade Wind-Tunnel (HGK)

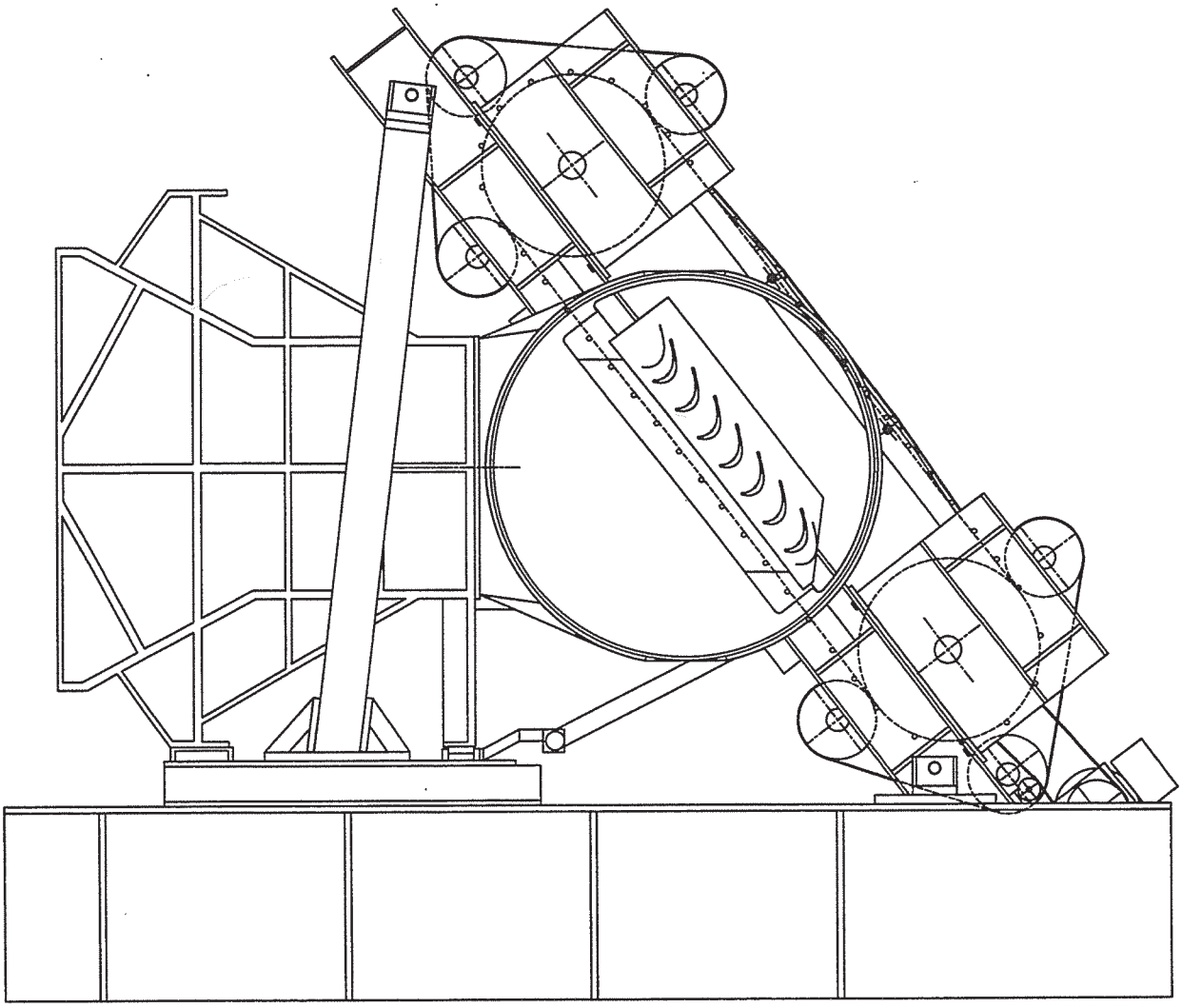

Fig.2 The generator of instationary flow conditions (EIZ) built in the HGK

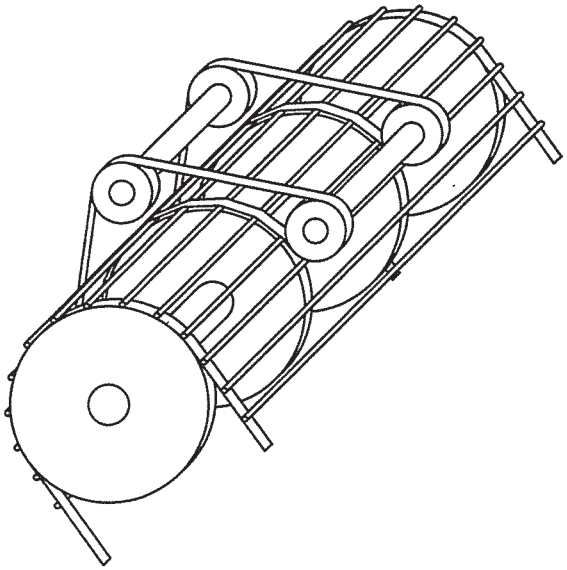

Fig.3 Mechanism for the reduction of the bar deflection around the main pulleys

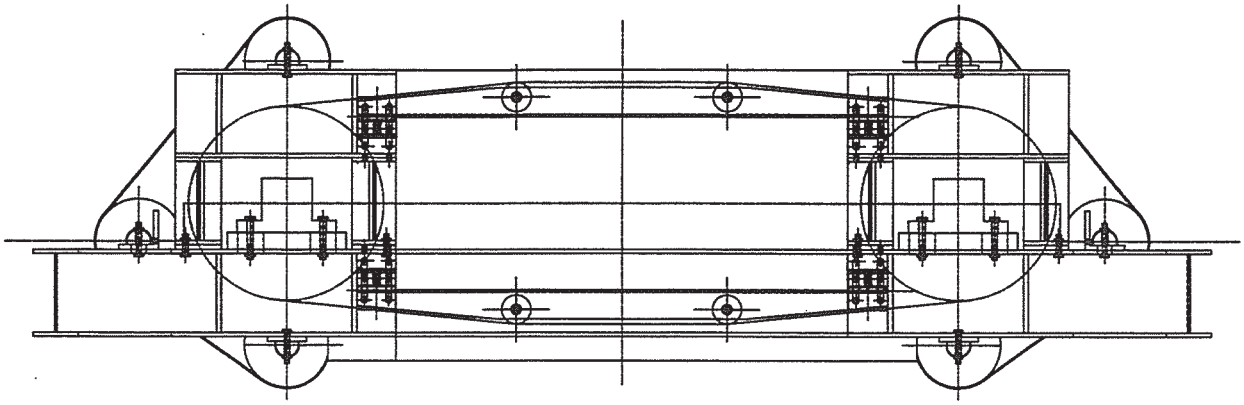

Fig.4 Stretch device for the belts to avoid flattering

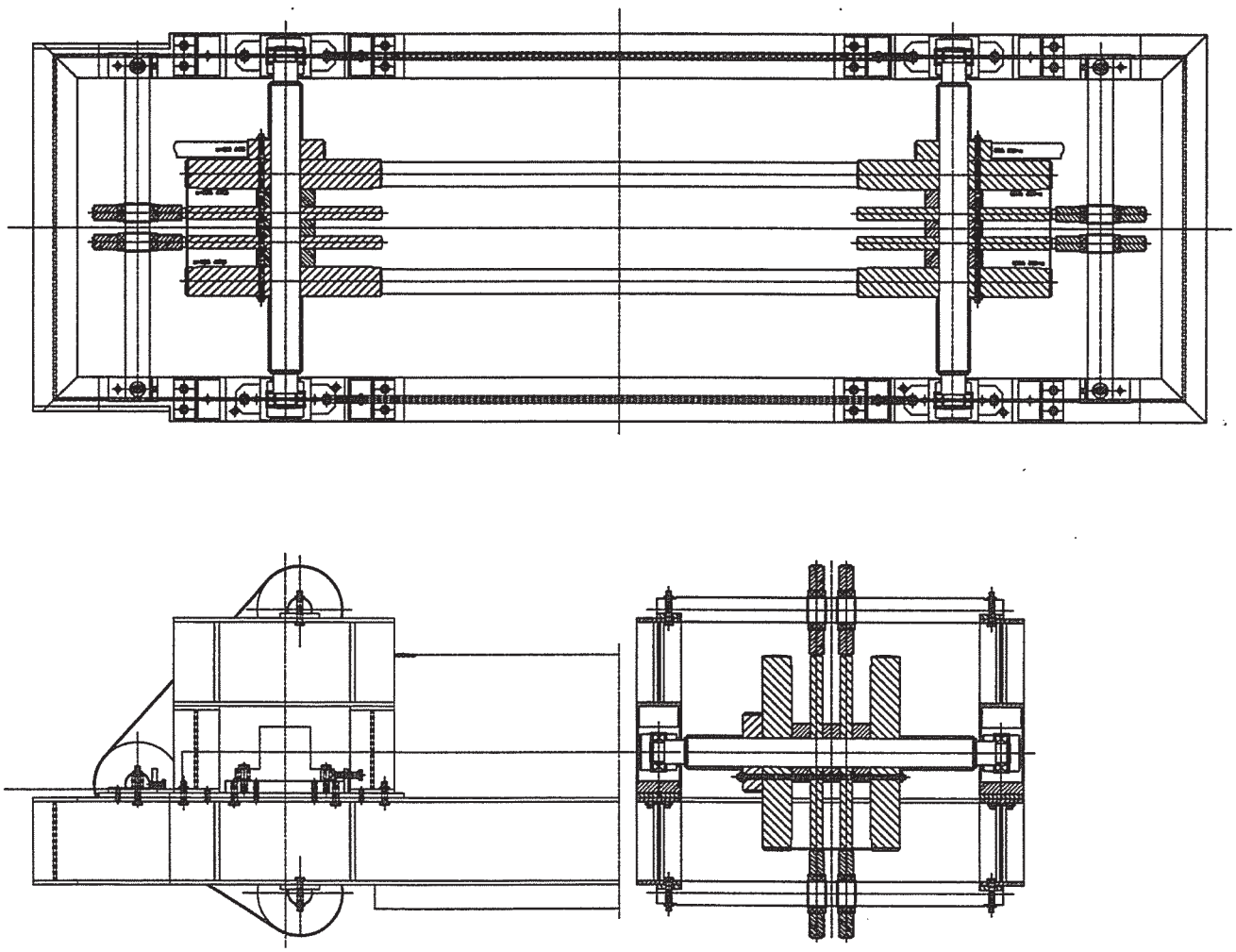

Fig.5 The main frame of the EIZ

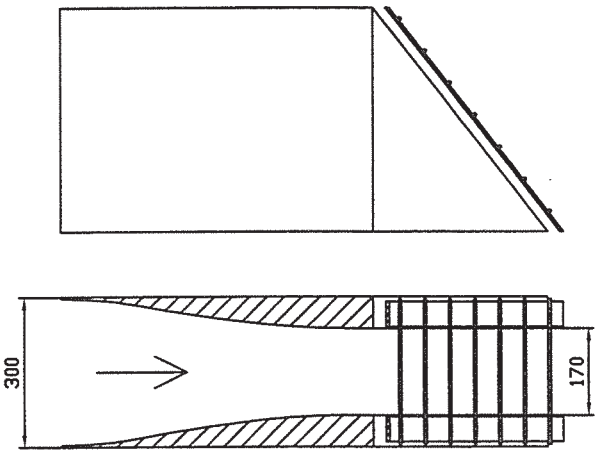

Fig.6 Sidewalls for the reduction of the test-section width upstream of the wake generator

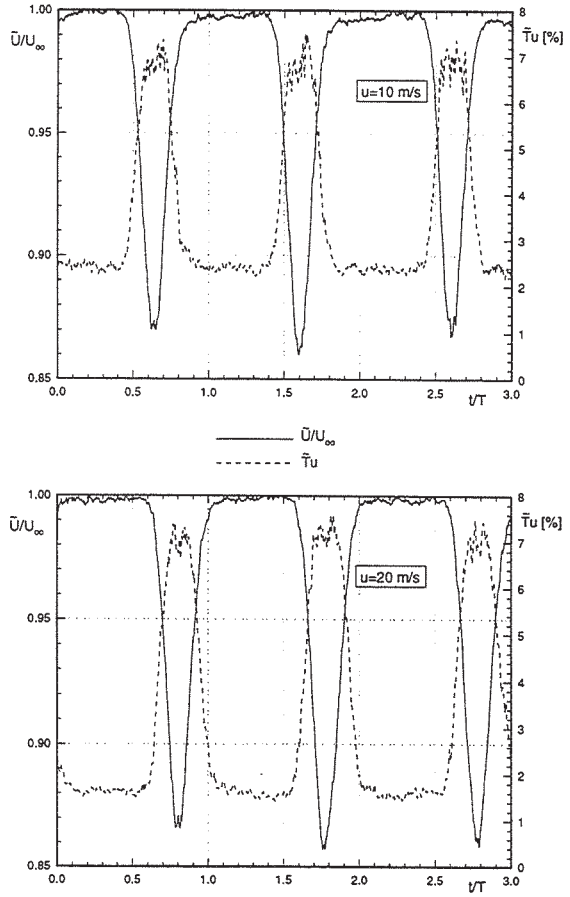

Fig.7 Ensemble averaged velocity and velocity fluctuations behind the moving bars (bar pitch t_b = 80 mm)

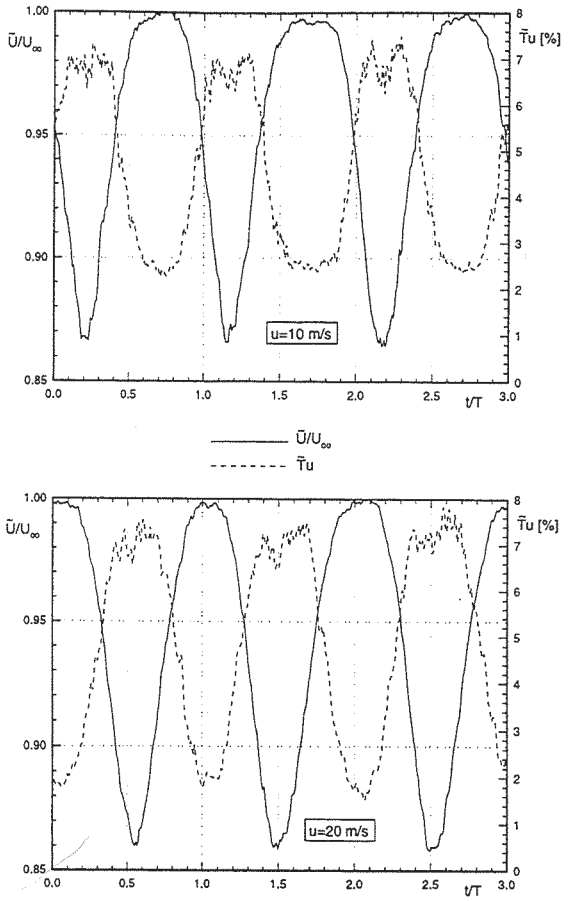

Fig.8 Ensemble averaged velocity and velocity fluctuations behind the moving bars (bar pitch t_b = 40 mm)

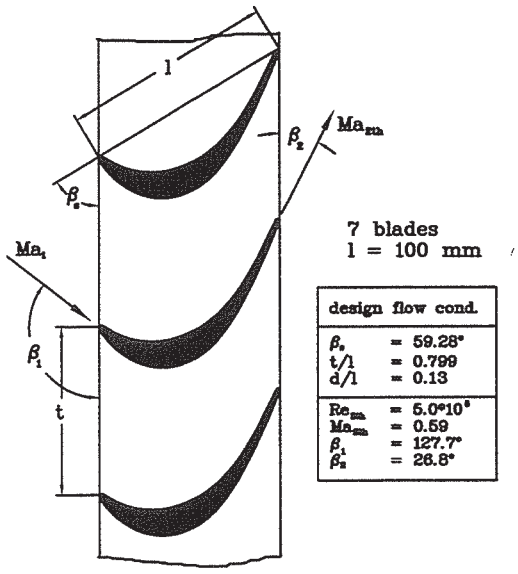

Fig.9 The turbine cascade T106

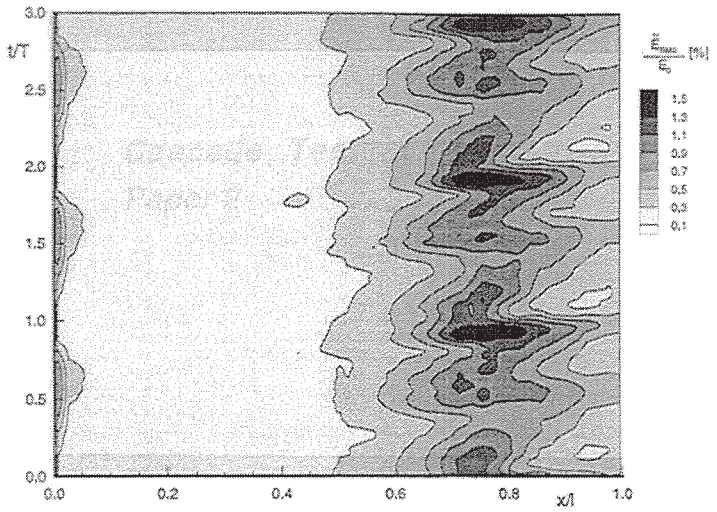

Fig.10 Ensemble averaged RMS of the hot film signals along the suction side of the profile T106 ($Ma_{2th} = 0.40$, $Re_{2th} = 2 \cdot 10^5$)

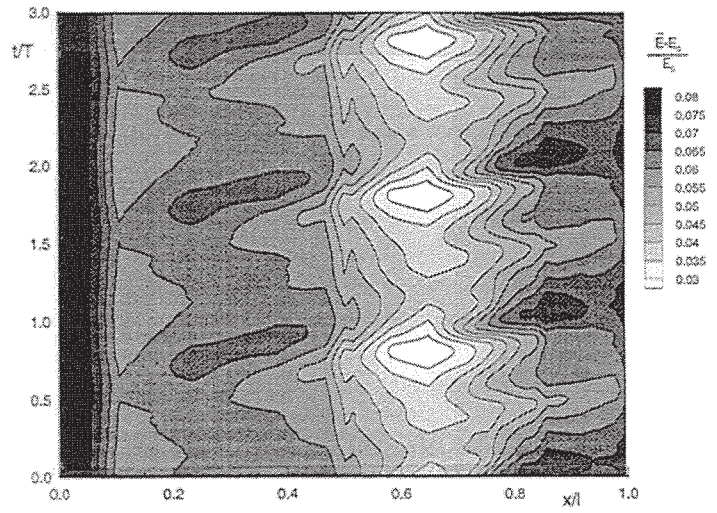

Fig.11 Ensemble averaged hot film signals along the suction side of the profile T106 ($Ma_{2th} = 0.40$, $Re_{2th} = 2 \cdot 10^5$)